



UWS Academic Portal

Ganoderma applanatum secondary metabolites induced apoptosis through different pathways

Elkhateeb, Waill A.; Zaghlol, Gihan M.; El-Garawani, Islam M.; Ahmed, Eman F.; Rateb, Mostafa E.; Abdel Moneim, Ahmed E.

Published in:
Biomedicine & Pharmacotherapy

DOI:
[10.1016/j.biopha.2018.02.058](https://doi.org/10.1016/j.biopha.2018.02.058)

Published: 01/05/2018

Document Version
Peer reviewed version

[Link to publication on the UWS Academic Portal](#)

Citation for published version (APA):

Elkhateeb, W. A., Zaghlol, G. M., El-Garawani, I. M., Ahmed, E. F., Rateb, M. E., & Abdel Moneim, A. E. (2018). Ganoderma applanatum secondary metabolites induced apoptosis through different pathways: in vivo and in vitro anticancer studies. *Biomedicine & Pharmacotherapy*, 101, 264-277. <https://doi.org/10.1016/j.biopha.2018.02.058>

General rights

Copyright and moral rights for the publications made accessible in the UWS Academic Portal are retained by the authors and/or other copyright owners and it is a condition of accessing publications that users recognise and abide by the legal requirements associated with these rights.

Take down policy

If you believe that this document breaches copyright please contact pure@uws.ac.uk providing details, and we will remove access to the work immediately and investigate your claim.

***Ganoderma applanatum* secondary metabolites induced apoptosis through different pathways: In vivo and in vitro anticancer studies**

**Waill A. Elkhateeb¹, Gihan M. Zaghlol², Islam M. EL-Garawani³, Eman.F.Ahmed^{1,*},
Mostafa E. Rateb⁴, Ahmed E. Abdel Moneim⁵**

¹Chemistry of Natural and Microbial Products Department, National Research Centre, Dokki-12311, Cairo, Egypt

²Botany and Microbiology Department, Faculty of Science, Helwan University, Cairo, Egypt

³Department of Zoology, Faculty of Science, Menoufia University, Menoufia, Egypt

⁴School of Science and Sport, University of the West of Scotland, Paisley PA1 2BE, UK

⁵Department of Zoology & Entomology, Faculty of Science, Helwan University, Cairo, Egypt

Abstract

Ganoderma applanatum is a widely distributed saprobic or parasitic mushroom, it was found at the bases of decaying logs in Hakozaki Higashi-ku Fukuoka-shi. Japan. The mushroom was extracted with 80% methanol, and LC-HRMS analysis was conducted to illustrate the bioactive ingredients. The cytotoxicity of the total metabolite extract was evaluated against human colon cancer cell line (Caco-2) which showed IC₅₀ value of 160±4.08 µg/ml. *G. applanatum* methanolic extract caused different morphological alterations and increased glutathione level in the treated cells. Interestingly, *G. applanatum* increased Bax/Bcl-2 ratio significantly ($P<0.05$) at concentrations of 80 and 160 µg/ml on Caco-2 undergoing apoptotic p53-independent pathway with low expression of p53 protein and up-regulated Cas-3 mRNA. The *in vivo* study on solid Ehrlich tumor (SEC) revealed a decrease in the volume of the developed tumor mass after five days of *G. applanatum* (200µg/ml) treatment. The apoptotic p53-dependant pathway was confirmed by mRNA Bax/Bcl-2 increased ratio in addition to p53 and Cas-3 up-regulation. In conclusion, *G. applanatum* could exert apoptotic antitumor properties in Caco-2 by p53-independent pathway and p53-dependant in SEC. The findings proved that *G. applanatum* can be a promising candidate as alternative or co-anticancer medications.

Keywords: *Ganoderma applanatum*, mushroom, anticancer, apoptosis, Caco-2, solid Ehrlich tumor.

Introduction

Cancer is one of the major human diseases and causes considerable suffering and economic loss worldwide. Colorectal cancer (CRC), with more than 750,000 deaths worldwide per year, is the third leading cause of cancer-related death in the Western world [1]. Chemotherapy counts more than 100 anticancer drugs with different mechanism of action [2]. Alarmingly, the current synthetic anti-cancer treatments available in market are not target specific and due to the increasing rate of mortality associated with cancer and toxic side effects of cancer chemo- and radiotherapies, which highlights the urgent need for new effective and less-toxic therapeutic drugs, discovery of new anticancer agents derived from nature has begun especially botanicals and the screening of natural products as a source of anticancer molecules especially those that have cytotoxic properties with minimal side effects [3]. Fourteen thousand kinds of mushrooms are recently known [4]. Many searches studied the use of mushroom extracts in cancer treatments to complement chemotherapy and radiation therapy by decreasing the side-effects of cancer, such as, anemia, nausea, bone marrow suppression, inflammation, and lowered resistance [5].

Antitumor bioactive compounds from mushrooms are of a significant importance. Recently, the anti-cancer agents include polysaccharides, proteins, fats, ash, glycosides, alkaloids, volatile oils, tocopherols, phenolics, flavonoids, carotenoids, folates, ascorbic acid enzymes, and organic acids. The active components in mushrooms responsible for conferring anti-cancer potential are polysaccharides, alkaloids, triterpenoids, polyphenols, etc [5]. Findings suggest that some mushrooms in combination with commercial anti-cancer drugs work have a synergetic effect in treating drug-resistant cancers [6]. Mushrooms are a source of antioxidants, anticancer, prebiotic, immunomodulating, anti-inflammatory, cardiovascular, anti-microbial, and hypoglycemic [7].

Ganoderma applanatum is a medicinal farming crop which grows within the dead and living trees. Studies proved this genus to have a potent antimicrobial, anti-fibrotic and anti-tumor properties [8]. Other effects are attributed to a wide variety of bioactive components, such as polysaccharides, triterpenes, sterols, lectins and other proteins [9-10]. This study was conducted to evaluate the antioxidative potential of the extract and the cytotoxicity of the bioactive compounds of this genus on colorectal cancer cell line, Caco-2 Human Colon Cancer, the inhibition of some anti-apoptosis proteins by affecting the regulation of the responsible genes

were also investigated. LC-HRMS analysis was used to evaluate the bioactive compounds and to investigate the significance of these metabolites in the biological activity.

Materials and methods

Collection and identification of mushroom

The mushroom was collected from the parks of Hakozaki Higashi-ku Fukuoka-shi. Japan. It was cut from the barks of dead trees and identified as *Ganoderma applanatum* by Mycological Society of Japan.

Extraction of mushroom metabolites

The mushroom was cut into small pieces and extracted with 80% methanol. The total extract was concentrated at 37°C by the use of a rotary evaporator.

LC-HRMS analysis

High resolution mass spectrometric data were obtained using a Thermo Instruments MS system (LTQ XL/LTQ Orbitrap Discovery) coupled to a Thermo Instruments HPLC system (Accela PDA detector, Accela PDA auto sampler, and Accela pump). The following conditions were applied: capillary voltage 45 V, capillary temperature 260°C, auxiliary gas flow rate 10-20 arbitrary units, sheath gas flow rate 40-50 arbitrary units, spray voltage 4.5 kV, mass range 100-2000 amu (maximum resolution 30000). For LC/MS, a Sunfire C18 analytical HPLC column (5 µm, 4.6 mm × 150 mm) was used with a mobile phase of 0 to 100% MeOH over 30 minutes at a flow rate of 1 ml.min⁻¹. The exact mass obtained for eluted peaks was used to deduce the possible molecular formulae for such mass, and these formulae were searched in Dictionary of Natural Products, CRC press, online version, for matching chemical structures. Analysis of data was performed using Xcalibur 3.0 and dereplication using dictionary of natural products database V. 23.1 on DVD.

In vitro study

Cell line maintenance and procedure

Human colon cancer cell line (Caco-2) was purchased from VACSRA, Egypt. 5×10⁵ cells were grown in 5 ml of complete growth medium (Lonza, Basel, Switzerland), RPMI-1640 medium supplemented with 10% fetal bovine serum, 1% (100 U/ml penicillin and 100 µg/ml streptomycin) at 37°C and 5% CO₂ in T25 tissue culture flasks. The medium was changed with new one every 48 hrs.

Evaluation of Cytotoxicity using neutral red uptake assay

When Caco-2 cells reached confluency, they were detached using 0.2% (w/v) trypsin and transferred to 96-cluster-well-culture plates at a concentration of 1×10^4 cells/well. Each well contained 100 μ l of cell suspension and the plates were incubated for 24 hrs to obtain a monolayer culture at 37°C under 5% CO₂. After the incubation period, the old media was removed and 100 μ l of medium free extract, serial dilutions of *G. applanatum* or 5-Fluorouracil (1.5 μ g/ml) as a standard treatment was added into 96-cluster-well-culture plates (8 wells/test material) and the Caco-2 cells were incubated at 37°C in a humidified 5% CO₂ incubator for 24 hrs. Next, Caco-2 cells were exposed to neutral red dye (4 mg/ml) for 3 hours in serum free medium after treatments incubation time. Cells were washed with PBS then distained using (50% EtOH and 5% glacial acetic acid in distilled water). The absorbance was measured at 540 nm using spectrophotometer (Hewlett Packard, USA) [11]. All determinations were performed in triplicates. Cell growth inhibitory rate was calculated in the following equation:

$$\text{Inhibition\%} = (1 - \text{Sample group OD/Control group OD}) \times 100$$

The maximal half inhibitory concentration (IC₅₀) of *G. applanatum* extract on Caco-2 cells was assessed as equivalent value of inhibitory curve.

For further investigations, Caco-2 cells were incubated with 3 μ l/ml DMSO, 1.5 μ g/ml of 5-Fluorouracil, IC₂₅ or IC₅₀ of *G. applanatum* extract for 24 hrs. Untreated group was served as a vehicle and the treatments were applied in triplicates.

Morphological Examination by phase contrast inverted microscopy

Treated cells and controls were examined for morphological changes using Olympus BX41 (Japan) with 400 \times magnification and then representative photos were digitally captured.

Acridine orange/ethidium bromide (AO/EB) dual fluorescent staining

To detect the evidence of apoptosis, necrosis and viability of cells, dual staining of cells by AO/EB was carried out. Five microliters of treated and control cultured cells were stained with 3 μ l of AO/EB stain (100 μ g/ml) and immediately examined using the fluorescent microscope (Olympus BX41, Japan). Five hundred cells were evaluated and then representative photos were digitally captured. Green colored cells with intact structure indicate viable cells, whereas cells with orange to red color were dead while apoptotic cells showed the blebbed cytoplasmic membrane and nuclear fragmentation.

Immunocytochemical staining

Cells were grown on coverslips and then they were incubated for 24 hrs with various treatments when reaching 70% confluency. Then, the treated and control cells were processed for immunocytochemical reaction using an avidin biotin complex immunoperoxidase technique. p53 nuclear protein in addition to Bcl-2 and Bax cytoplasmic markers for apoptosis were detected using an anti-human p53, Bcl-2 and Bax monoclonal antibodies (Glostrup, Hovedstaden, Denmark). Additionally, nuclear proliferating antigen (Ki-67) immune reaction was evaluated also as a marker of cell proliferation using an anti-human Ki-67 monoclonal antibody (Glostrup, Hovedstaden, Denmark). Cells were examined blindly and fields were chosen randomly. Five fields per slide were scored. The mean percentage of positive cells in all groups was used as immunocytochemical scoring system (positive cells/total number of counted cells) $\times 100$. Cells were examined (400 \times) using light microscope (Olympus BX 41, Japan) and representative photos were digitally captured.

In vivo study

Ehrlich tumor

The Ehrlich ascitic tumor, derived from a spontaneous murine mammary adenocarcinoma was maintained in ascitic form by passages in Swiss mice by weekly intraperitoneal transplantation of 10^6 tumor cells. The ascitic fluid was collected by intraperitoneal puncture using a sterile insulin syringe. Ascitic tumor cell counts were done in a Neubauer hemocytometer. The cells were found to be more than 99% viable using trypan blue dye exclusion method [12]. A model of solid Ehrlich carcinoma (SEC) was used in this study, where 2.5×10^6 of the Ehrlich carcinoma cells (ECC) obtained from the Pharmacology and Experimental Oncology Unit of the National Cancer Institute, Cairo University, Egypt, were implanted subcutaneously into the right thigh of the hind limb of mice.

Animals and experimental design

Female Swiss albino mice, 8 to 12 weeks old, weighing 25.9 ± 2.4 g were housed in plastic cages at room temperature (20 ± 2 °C) in a 12-hrs light/dark cycle and free access to food and water in animal house of National Organization for Drug Control and Research.

Animals (6 mice/group) were divided into three groups (Untreated control, 5-Fluorouracil, injected intraperitoneally at 20 mg/kg body weight and *G. applanatum* extract administered orally at 200 mg/kg body weight). After four days of tumor inoculation, the different treatments were

continued for five days. The experiments were conducted according to the National Research Council's guidelines.

Assessment of the tumor volume (TV) of SEC

Tumor volume was measured after the 1st and 5th days of different treatments, using a Vernier caliper (Tricle, China). The volume of developed tumor mass was calculated by the following formula:

$$TV (\text{mm}^3) = 4\pi (A/2)^2 \times (B/2)$$

Where A is the minor tumor axis; B the major tumor axis and π equals to 3.14 [12].

Histological changes in SEC tissues

The tumor was fixed in 10% neutral buffered formalin for 24 hrs, dehydrated in ethyl alcohol, cleared in xylene, and mounted in molten paraplast. Sections of 4–5 μm were obtained from the prepared blocks and stained with hematoxylin-eosin. Sections were examined using (Olympus BX 41, Japan) microscope.

Immunohistochemical staining of SEC tissues

Tissue samples were fixed in neutral buffered formalin (10%), embedded in paraffin, and sectioned into 4 μm sections. Immunocytochemical reactions were performed using the peroxidase/anti-peroxidase (PAP) method [13]. Samples were analyzed using Image J software and the score was divided into four groups based on the percentage of positively stained tumor cells as follows: 0 (negative expression, 0% - 15%); 1+ (weak expression, 16% - 30%); 2+ (moderate expression, 31% - 60%) and 3+ (strong expression, 61% - 100%).

Oxidative stress markers

Lipid peroxidation (LPO) in the Caco-2 cells as well as SEC tissue homogenate was determined as described by [14]. The level of nitric oxide (NO) in the homogenate was evaluated as previously reported by [15]. Whereas, the level of glutathione (GSH) was investigated according to the method of [16].

Quantitative real time PCR

Total RNA was purified from the Caco-2 cells as well as SEC tissue using an RNeasy Plus Minikit (Qiagen, Valencia, CA). cDNA was prepared using the RevertAid™ H Minus Reverse Transcriptase (Fermentas, Thermo Fisher Scientific Inc., Canada). The cDNA samples were run in triplicate for real-time PCR analysis. Real-time PCR reactions were performed using Power SYBR® Green (Life Technologies, CA) on an Applied Biosystems 7500 system. Relative values

of gene expression were normalized to GAPDH. Primer sequences and accession numbers of the genes are provided in Table (1).

Statistical analysis

All results were expressed as the mean \pm standard deviation. Data for multiple variable comparisons were analyzed by one-way analysis of variance (ANOVA). For the comparison of significance between groups, Duncan's test was used as a post hoc test, and probability level of ($P<0.05$) was considered significant.

Results

LC-HRMS analysis of G. applanatum extract

LC-HRMS analysis of *G. applanatum* methanolic extract revealed the presence of 47 metabolites (Table 2). Tentative identification of the quasi-molecular ion peaks and their molecular formulae indicated 45 known metabolites and 2 potentially new compounds where no natural hits was found for such formulae at the Dictionary of Natural products database. The identified compounds represent different chemical classes of natural products such as terpenes and polyketides, which represented the majority of the identified compounds, alkaloids, xanthenes, isocoumarins, dibenzofurans, and peptides. Although about 15 of the identified compounds don't possess any reported biological activity, 11 of the identified metabolites reported to have strong anticancer effect, some with antibacterial, antifungal, antiviral, anti-inflammatory, and antioxidant effects.

In vitro study results

Assessment of cytotoxicity in Caco-2 cells

The inhibitory effect of *G. applanatum* on Caco-2 cells after 24 hrs of incubation was assessed by neutral red uptake assay and the half maximal inhibitory concentration (IC₅₀) value was 160±4.08 µg/ml (Figure 1). The inverted phase contrast observation also revealed the presence of cellular shrinkage and irregular shape appearance with *G. applanatum* incubations (Figure 2).

Assessment of viability and morphological changes by acridine orange/ethidium bromide (AO/EB) dual fluorescent staining in Caco-2 cells

Basic morphological changes in apoptotic cells can be detected by AO/EB dual fluorescent staining. Furthermore, it allows for the distinction between normal cells, early and late apoptotic cells, and necrotic cells. Therefore, AO/EB staining is a new qualitative and quantitative method to examine apoptosis [17]. Morphological features of apoptosis such as cytoplasmic membrane blebbing, chromatin condensation, nuclear fragmentation, shrinkage of cells were evaluated by fluorescent microscopy. The results showed statistically significant ($P < 0.05$) dose dependant alterations in treated Caco-2 cells when compared with the control cells which exhibited normal intact morphology with bright green staining (Figure 2).

Immunocytochemical assessment of p53, Bcl-2 and Ki-67 protein expression in Caco-2 cells

The expression of cytoplasmic Bcl-2 (anti-apoptotic protein) and nuclear Ki-67 (proliferation protein marker) were detected immunocytochemistry (Figure 2). The count of positive stained

cells of both markers revealed statistically significant ($P<0.05$) dose dependant down-expression in Caco-2 cells after *G. applanatum* (80 and 160 $\mu\text{g/ml}$) incubations (Figure 3). On the contrary, p53 (tumor suppressor protein) immuno-staining revealed negative reactivity in both control and treated cells.

Quantitative real time PCR (qPCR) for Bcl-2, Bax and Cas-3 expression in Caco-2 cells

In order to quantify the expression of Bcl-2, Bax and Cas-3 as apoptosis-related genes, the number of mRNA copies was evaluated by qPCR and the results were calculated based on calibration curve for corresponding GAPDH values. *G. applanatum* (80 and 160 $\mu\text{g/ml}$) induced statistically significant ($P<0.05$) dose dependant down-regulation of Bcl-2 gene (Figure 4), while dose dependent up-regulation of Bax and Cas-3, from four to more than fivefold changes respectively, were countered in Caco-2 cells after 24 hrs of incubation. Moreover, the Bax/Bcl-2 ratio has the tendency to increase significantly when compared with control (Figure 4).

Assessment of oxidative status in Caco-2 cells

Incubation of *G. applanatum* extract with Caco-2 cells for 24 hrs revealed statistically non significant ($P<0.05$) changes in lipid peroxidation and nitric oxide levels with respect to the control values. However, the level of glutathione showed statistically significant ($P<0.05$) dose dependent elevation after *G. applanatum* incubation. In contrast, 5-FU caused significant decrease in GSH levels (Figure 5).

In vivo study results

Assessment of solid Ehrlich tumor volume

The effect on tumor growth inhibition was evaluated as the volume of developed tumor mass on the 9th day after ECC cells implantation which showed significant ($P<0.05$) tumor growth inhibition, as measured as volume change, after five days of *G. applanatum* (200 $\mu\text{g/ml}$) treatment when compared with the control ESC group (Figure 6).

Assessment of oxidative status in solid Ehrlich tumor tissues

Lipid peroxidation, nitric oxide and glutathione levels were estimated in SEC tissue. The obtained results illustrated that *G. applanatum* (200 $\mu\text{g/ml}$) caused statistically significant elevation ($P<0.05$) in GSH levels with respect to the control values. However, *G. applanatum* treatment decreased the level of LPO (Figure 7).

Histological changes in SEC tissues

Concerning histological observations, the SEC showed more abundant necrotic lesions in *G. applanatum* treated group, with some occasional residual SEC cells, in addition to the appearance of shrunk cells around the necrotic areas. 5-Fluorouracil treated groups showed less alteration than that of the tested extract group, while the untreated group showed normal tumor architecture (Figure 8).

Immunohistochemical assessment of p53, Bax and Bcl-2 expression in SEC tissues

Tumor suppressor protein, p53, was elevated significantly ($P<0.05$) in the treated groups with respect to the control values. Additionally, immunohistochemical localization of Bax protein showed significant elevation ($P<0.05$) when compared with the control sections (Figure 9). On the other hand, Bcl-2 as an anti-apoptotic marker, exhibited less positive immune-reactivity with cytoplasmic brown stain development (Figure 8). Moreover, the apoptotic efficacy of the examined extract was also proved by calculating Bax/Bcl-2 ratio which has the tendency to increase significantly ($P<0.05$), about threefold with respect to the control (Figure 9).

Quantitative real time PCR for Bcl-2, Bax and Cas-3 expression in SEC tissues

The expression of several apoptosis related genes, Bcl-2, Bax and Cas-3, were relatively quantified as mRNA levels to investigate the molecular mechanism of antitumor properties of *G. applanatum* on ESC tissues. However, Bax and Cas-3 up-regulation was significantly ($P<0.05$) recorded while the Bcl-2 expression revealed down-regulation in *G. applanatum* (200 $\mu\text{g/ml}$) group when compared with control. Bax/Bcl-2 ratio tends to increase with nine fold higher than that of the control (Figure 10).

Discussion

The main objective of this work was to study the potential anticancer activity of *G. applanatum* *in vitro* against Caco-2 cancer cell line and *in vivo* against murine solid tumor induced in mice. Reports have described interesting anticancer properties of mushroom [18-19]. According to Akindele et al. [20] patients may turn to integrative therapies when the disease they are battling does not respond to synthetic medical therapies and/or to help reduce symptoms. From previous studies, some mushrooms such as maitake mushroom (*Grifola frondosa*) has been found to fight cancer via different routes [21].

LC-HRMS analysis of *G. applanatum* extract revealed the presence of 47 metabolites representing different chemical classes of natural products mainly terpenoids and polyketides. About 11 of the identified metabolites reported to have strong anticancer effect through different mechanisms, some with anti-inflammatory and antioxidant effects which would support the overall cytotoxic effect of the extract. Additionally, about 15 of the identified compounds don't possess any reported biological activity, and they could have a potential in the cytotoxic effect exhibited by this extract. This would require more in-depth study. Applanoxidic acids A-H are a group of triterpenes which reported to have strong antitumor and antioxidant effect. It was reported that polysaccharides previously isolated from *G. applanatum* have strong cytotoxic effect [22]. However, the way of extract preparation either doesn't allow for polysaccharide extraction or the presence of high molecular weight polysaccharides which were not detected by the range of accurate mass used in our LCMS analysis. This could allow us to propose the cytotoxic effect of *G. applanatum* extract in this study was due to other naturally occurring metabolites in the methanolic extract. Hence, *G. applanatum* may have a cancer preventive effect and we found that *G. applanatum* concentration-dependently inhibited cell viability and exhibited apoptosis *in vivo* and *in vitro*. In Caco-2 cells, mushroom inhibited cell viability with an IC₅₀ of approximately 160 µg/ml after 24 hrs incubation. The results suggest that *G. applanatum* caused cytotoxicity in Caco-2 cells.

Oxidative stress played a crucial role in tumor progress. *G. applanatum* in the current study was showed antioxidant effect as evidenced by a significant reduction in lipid peroxidation and the production of pro-inflammatory marker, NO. It was reported that the production of NO in tissues could contribute to the carcinogenesis process [23] because overproduction of NO could lead to enhanced replication of genes and oxidative damage to DNA. Whereas, cancerous cells demand

high ROS concentrations in order to maintain their high proliferation rate [24]. In the current experiment, *G. applanatum* not only significantly restrained lipid peroxidation and NO production, but also effectively increased the antioxidant defense system and exerted cytotoxicity against caco-2 cancer cells and murine solid tumor induced in mice. The results obtained in the present work suggest that some compounds present in the tested mushroom can restrain the cascade of events that takes place in oxidative stress.

In cancer study, imbalance between oxidant and antioxidant molecules in cancer cells is serious for expecting whether cancer progression can be suppressed. For this reason, this study investigated the effect of mushroom on antioxidant enzyme levels. The level of oxidative stress markers, such as lipid peroxidation and glutathione are important indicators for cellular responses to various oxidative stresses [25]. A moderate increase in ROS can promote cell proliferation and differentiation. The increase of ROS production may depend on diverse mechanisms, such as the activation of oncogenes, aberrant metabolism, mitochondrial dysfunction, and loss of functional p53 [26]. Lipid peroxidation prevention and robust antioxidant system may be a valuable approach for cancer prevention and treatment [27].

In the present study, we investigated the mRNA expression of caspase3, Bax and Bcl-2 and we found that mushroom was able to up-regulated caspases-3 and Bax along with down-regulating Bcl-2 expression. The test results led us to investigate the modulation of p53 protein and cell cycle arrest of cancer cells after administration of the mushroom. Up-regulation of p53 protein associated with cell cycle arrest at sub-G1 stage clearly points out the actual cause of drug induced DNA damage [28]. The over-expression of apoptotic protein Bax, the lower-expression of antiapoptotic protein Bcl-2 clearly indicates that there were considerable changes in the balance of this protein ratio which triggered the beginning of the apoptotic process [28]. Bax/Bcl-2 ratio is a cell death switch in response to apoptotic stimuli. The elevation in Bax/Bcl-2 ratio participates to the release of cytochrome *C* from mitochondria and activates the intrinsic mitochondrial apoptotic pathway. As a result, change in Bax and Bcl-2 expression determines cell susceptibility to apoptotic stimuli. An increased Bax/Bcl-2 ratio can activate caspase-3 and result in apoptosis [29]. Administration of *G. applanatum* to Caco-2 cells and murine mice with mushroom significantly increased the Bax and decreased the Bcl-2 mRNA and protein expressions. The altered ratio of pro-apoptotic and anti-apoptotic factors favored the promotion of apoptosis. Therefore, mushroom reduced the ability of Bcl-2 to bind to Bax and enhanced the

translocation of Bax from cytosol to mitochondria, further increasing the susceptibility of the cells to apoptosis [28]. The obtained findings demonstrated the ability of mushroom to induce apoptosis.

In the current study, *G. applanatum* showed potent anticancer effect *in vivo* and *in vitro* with different pathways. The compounds of mushroom extract may be metabolized by the mice leading to generation of different bioactive compounds or the metabolism may activate some compounds of mushroom that are inactive in the cell culture conditions. Furthermore, these metabolites may enhance expression of some silenced genes as resulted in p53 mRNA of mice solid tumor in the current study. All these suggestions could support the different level of tumor growth inhibitory effects. In conclusion, the more inhibitory effect of mushroom on tumor growth *in vivo* might be caused by some more effective metabolites of mushroom. Future research to explore the metabolism of mushroom extract is needed to clarify the impact of biotransformation on the efficacy of *G. applanatum* extracts *in vivo*.

Acknowledgements

We thank Prof. Marcel Jaspars, the Marine Biodiscovery Centre, University of Aberdeen, for acquiring LC-HRMS.

References

- [1] W.H.O. WHO, WHO Cancer Fact sheet, 2017. <http://www.who.int/mediacentre/factsheets/fs297/en/>.
- [2] S. Dasari, P.B. Tchounwou, Cisplatin in cancer therapy: molecular mechanisms of action, *Eur J Pharmacol* 740 (2014) 364-78.
- [3] L. Pan, H.B. Chai, A.D. Kinghorn, Discovery of new anticancer agents from higher plants, *Front Biosci (Schol Ed)* 4 (2012) 142-56.
- [4] M.E. Valverde, T. Hernandez-Perez, O. Paredes-Lopez, Edible mushrooms: improving human health and promoting quality life, *Int J Microbiol* 2015 (2015) 376387.
- [5] S. Patel, A. Goyal, Recent developments in mushrooms as anti-cancer therapeutics: a review, *3 Biotech* 2(1) (2012) 1-15.
- [6] X.J. Luo, L.L. Li, Q.P. Deng, X.F. Yu, L.F. Yang, F.J. Luo, L.B. Xiao, X.Y. Chen, M. Ye, J.K. Liu, Y. Cao, Grifolin, a potent antitumour natural product upregulates death-associated protein kinase 1 DAPK1 via p53 in nasopharyngeal carcinoma cells, *Eur J Cancer* 47(2) (2011) 316-25.
- [7] C. Sarikurku, B. Tepe, M. Yamac, Evaluation of the antioxidant activity of four edible mushrooms from the Central Anatolia, Eskisehir - Turkey: *Lactarius deterrimus*, *Suillus collitinus*, *Boletus edulis*, *Xerocomus chrysenteron*, *Bioresour Technol* 99(14) (2008) 6651-5.
- [8] Q. Luo, L. Di, W.F. Dai, Q. Lu, Y.M. Yan, Z.L. Yang, R.T. Li, Y.X. Cheng, Applanatumin A, a new dimeric meroterpenoid from *Ganoderma applanatum* that displays potent antifibrotic activity, *Org Lett* 17(5) (2015) 1110-3.
- [9] I.C. Ferreira, S.A. Heleno, F.S. Reis, D. Stojkovic, M.J. Queiroz, M.H. Vasconcelos, M. Sokovic, Chemical features of *Ganoderma* polysaccharides with antioxidant, antitumor and antimicrobial activities, *Phytochemistry* 114 (2015) 38-55.
- [10] J.Q. Ma, C.M. Liu, Z.H. Qin, J.H. Jiang, Y.Z. Sun, *Ganoderma applanatum* terpenes protect mouse liver against benzo(alpha)pyren-induced oxidative stress and inflammation, *Environ Toxicol Pharmacol* 31(3) (2011) 460-8.
- [11] W.S. Stokes, S. Casati, J. Strickland, M. Paris, Neutral red uptake cytotoxicity tests for estimating starting doses for acute oral toxicity tests, *Curr Protoc Toxicol* Chapter 20 (2008) Unit 20 4.

- [12] F.M. Metwally, H.A. El-Mezayen, A.E. Abdel Moneim, N.E. Sharaf, Anti-Tumor Effect of *Azadirachta indica* (Neem) on Murine Solid Ehrlich Carcinoma, *Acad J Cancer Res* 7(1) (2014) 38-45.
- [13] L.A. Sternberger, *Immunocytochemistry*, 2d ed., Wiley, New York, 1979.
- [14] H. Ohkawa, N. Ohishi, K. Yagi, Assay for lipid peroxides in animal tissues by thiobarbituric acid reaction, *Anal Biochem* 95(2) (1979) 351-8.
- [15] L.C. Green, D.A. Wagner, J. Glogowski, P.L. Skipper, J.S. Wishnok, S.R. Tannenbaum, Analysis of nitrate, nitrite, and [¹⁵N]nitrate in biological fluids, *Anal Biochem* 126(1) (1982) 131-8.
- [16] G.L. Ellman, Tissue sulfhydryl groups, *Arch Biochem Biophys* 82(1) (1959) 70-7.
- [17] K. Liu, P.C. Liu, R. Liu, X. Wu, Dual AO/EB staining to detect apoptosis in osteosarcoma cells compared with flow cytometry, *Med Sci Monit Basic Res* 21 (2015) 15-20.
- [18] A. Rosa, M. Nieddu, A. Piras, A. Atzeri, D. Putzu, A. Rescigno, Maltese mushroom (*Cynomorium coccineum* L.) as source of oil with potential anticancer activity, *Nutrients* 7(2) (2015) 849-64.
- [19] P. Zucca, A. Rosa, C.I. Tuberoso, A. Piras, A.C. Rinaldi, E. Sanjust, M.A. Dessi, A. Rescigno, Evaluation of antioxidant potential of "maltese mushroom" (*Cynomorium coccineum*) by means of multiple chemical and biological assays, *Nutrients* 5(1) (2013) 149-61.
- [20] A.J. Akindele, Z.A. Wani, S. Sharma, G. Mahajan, N.K. Satti, O.O. Adeyemi, D.M. Mondhe, A.K. Saxena, In Vitro and In Vivo Anticancer Activity of Root Extracts of *Sansevieria liberica* Gerome and Labroy (Agavaceae), *Evid Based Complement Alternat Med* 2015 (2015) 560404.
- [21] N. Kodama, K. Komuta, H. Nanba, Effect of Maitake (*Grifola frondosa*) D-Fraction on the activation of NK cells in cancer patients, *J Med Food* 6(4) (2003) 371-7.
- [22] M. Osinska-Jaroszuk, M. Jaszek, M. Mizerska-Dudka, A. Blachowicz, T.P. Rejczak, G. Janusz, J. Wydrych, J. Polak, A. Jarosz-Wilkolazka, M. Kandefer-Szerszen, Exopolysaccharide from *Ganoderma applanatum* as a promising bioactive compound with cytostatic and antibacterial properties, *Biomed Res Int* 2014 (2014) 743812.
- [23] L. Ma, H. Chen, P. Dong, X. Lu, Anti-inflammatory and anticancer activities of extracts and compounds from the mushroom *Inonotus obliquus*, *Food Chemistry* 139(1) (2013) 503-508.

- [24] V. Sosa, T. Moline, R. Somoza, R. Paciucci, H. Kondoh, L.L. ME, Oxidative stress and cancer: an overview, *Ageing Res Rev* 12(1) (2013) 376-90.
- [25] U.K. Udensi, P.B. Tchounwou, Dual effect of oxidative stress on leukemia cancer induction and treatment, *J Exp Clin Cancer Res* 33 (2014) 106.
- [26] G. Barrera, Oxidative stress and lipid peroxidation products in cancer progression and therapy, *ISRN Oncol* 2012 (2012) 137289.
- [27] H. Zhong, H. Yin, Role of lipid peroxidation derived 4-hydroxynonenal (4-HNE) in cancer: focusing on mitochondria, *Redox Biol* 4 (2015) 193-9.
- [28] T. Li, N. Kon, L. Jiang, M. Tan, T. Ludwig, Y. Zhao, R. Baer, W. Gu, Tumor suppression in the absence of p53-mediated cell-cycle arrest, apoptosis, and senescence, *Cell* 149(6) (2012) 1269-83.
- [29] T.T. Renault, O. Tejjido, B. Antonsson, L.M. Dejean, S. Manon, Regulation of Bax mitochondrial localization by Bcl-2 and Bcl-x(L): keep your friends close but your enemies closer, *Int J Biochem Cell Biol* 45(1) (2013) 64-7.
- [30] C.C. Wang, H.Z. Liu, M. Liu, Y.Y. Zhang, T.T. Li, X.K. Lin, Cytotoxic metabolites from the soil-derived fungus *Exophiala pisciphila*, *Molecules* 16(4) (2011) 2796-801.
- [31] C. Valdivia, M. Kettering, H. Anke, E. Thines, O. Sterner, Diterpenoids from *Coprinus heptemerus*, *Tetrahedron* 61(40) (2005) 9527-9532.
- [32] A. Evidente, L. Sparapano, G. Bruno, A. Motta, Sphaeropsidins D and E, two other pimarane diterpenes, produced in vitro by the plant pathogenic fungus *Sphaeropsis sapinea* f. sp. *cupressi*, *Phytochemistry* 59(8) (2002) 817-23.
- [33] D.B. Stierle, A.A. Stierle, T. Girtsman, K. McIntyre, J. Nichols, Caspase-1 and -3 inhibiting drimane sesquiterpenoids from the extremophilic fungus *Penicillium solitum*, *J Nat Prod* 75(2) (2012) 262-6.
- [34] F. León, M. Valencia, A. Rivera, I. Nieto, J. Quintana, F. Estévez, J. Bermejo, Novel Cytostatic Lanostanoid Triterpenes from *Ganoderma australe*, *Helvetica Chimica Acta* 86(9) (2003) 3088-3095.
- [35] T. Lin, X. Lin, C.-H. Lu, Y.-M. Shen, Three New Triterpenes from Xylarialean sp. A45, an Endophytic Fungus from *Annona squamosa* L, *Helvetica Chimica Acta* 94(2) (2011) 301-305.

- [36] Z.X. Xia, D.D. Zhang, S. Liang, Y.Z. Lao, H. Zhang, H.S. Tan, S.L. Chen, X.H. Wang, H.X. Xu, Bioassay-guided isolation of prenylated xanthenes and polycyclic acylphloroglucinols from the leaves of *Garcinia nuijiangensis*, *J Nat Prod* 75(8) (2012) 1459-64.
- [37] S.J. Wu, Y.L. Leu, C.H. Chen, C.H. Chao, D.Y. Shen, H.H. Chan, E.J. Lee, T.S. Wu, Y.H. Wang, Y.C. Shen, K. Qian, K.F. Bastow, K.H. Lee, Camphoratins A-J, potent cytotoxic and anti-inflammatory triterpenoids from the fruiting body of *Taiwanofungus camphoratus*, *J Nat Prod* 73(11) (2010) 1756-62.
- [38] S.M. Chairul, Y. Hayashi, Lanostanoid triterpenes from *Ganoderma applanatum*, *Phytochemistry* 35(5) (1994) 1305-1308.
- [39] K. Watanabe, T. Ohtsuki, Y. Yamamoto, M. Ishibashi, New Kehokorins and Trichiols from the Myxomycete *Trichia favoginea*, *Heterocycles* 71(8) (2007) 1807-1814.

Figure legends

Figure 1. *In vitro* cytotoxicity activity of the *G. applanatum* extract on Human colon cancer cell line (Caco-2) after exposure to the extract for 24 hrs.

Data represents means of three independent experiments; bars, standard deviation and a: significant with respect to the control ($P<0.05$). 5-FU: 5-Fluorouracil (1.5 $\mu\text{g/ml}$).

Figure 2. Representative photomicrographs of control and treated Caco-2 cells after 24 hrs. Morphological changes as observed by inverted microscope (phase contrast); viability, mode and stages of cell death as detected by acridine orange/ethidium bromide (AO/EB) dual fluorescent staining show the development of membrane blebbing (white arrows) and apoptotic nuclear fragmentation as hallmark of apoptotic mode of death, reddish necrotic nuclei and intact green viable cells; protein expression as evaluated by immunocytochemical reactivity, Bcl-2 (-ve cells, black arrows), Ki-67 (-ve cells, red arrows) and p53 (-ve with all treatments). 5-FU: 5-Fluorouracil (1.5 $\mu\text{g/ml}$), G.a: *G. applanatum*.

Figure 3. Effect of *G. applanatum* on the percentage of positively stained cells of Bcl-2 and Ki-67 detected by immunocytochemistry in control and treated Caco-2 cells after 24 hrs.

Data represents means of ten different fields; bars, standard deviation and a: significant with respect to the control ($P<0.05$). 5-FU: 5-Fluorouracil (1.5 $\mu\text{g/ml}$).

Figure 4. Effect of *G. applanatum* on the relative mRNA alterations of Bax, Cas-3 and Bcl-2 expression, and Bax/Bcl-2 ratio in Caco-2 cells.

Data represented the average of three replicates; bars, standard deviation and a: significant with respect to the control ($P<0.05$). 5-FU: 5-Fluorouracil (1.5 $\mu\text{g/ml}$).

Figure 5. Effect of *G. applanatum* on lipid peroxidation (LPO), nitric oxide (NO) and glutathione (GSH) levels in Caco-2 cells after 24 hrs.

Data represents means of three independent experiments; bars, standard deviation and a: significant with respect to the control ($P<0.05$). 5-FU: 5-Fluorouracil (1.5 $\mu\text{g/ml}$).

Figure 6. Effect of *G. applanatum* on the solid Ehrlich tumor volume after five days of treatment.

Data represents means ($n= 5$); bars, standard deviation and a: significant with respect to the control ($P<0.05$). 5-FU: 5-Fluorouracil (20 mg/kg, i.p.).

Figure 7. Effect of *G. applanatum* on lipid peroxidation (LPO), nitric oxide (NO) and glutathione (GSH) levels in solid Ehrlich tumor tissues after 4 days of treatment.

Data represents means (n= 5); bars, standard deviation and a: significant with respect to the control ($P<0.05$). 5-FU: 5-Fluorouracil (20 mg/kg, i.p.).

Figure 8. Representative photomicrographs of control and treated solid Ehrlich tumor sections taken from the different treatment group and stained by H&E showing extensive necrotic areas (N); Bcl-2 and Bax protein expression as detected by immunohistochemistry show more positive reactivity with increased brown color development as cytoplasmic localization while p53 expression as nuclear localization. 5-FU: 5-Fluorouracil (20 mg/kg, i.p.), G.a: *G. applanatum*.

Figure 9. Effect of *G. applanatum* on the percentage of positively stained cells of Bcl-2, Bax and p53 as detected by immunocytochemistry in control and treated mice-bearing SEC tissues (left panel). Effect of *G. applanatum* on Bax/Bcl-2 ratio (right panel).

Data represents means of ten different fields; bars, standard deviation and a: significant with respect to the control ($P<0.05$). 5-FU: 5-Fluorouracil (20 mg/kg, i.p.).

Figure 10. Effect of *G. applanatum* on the relative mRNA expression of Bax, Cas-3 and Bcl-2, and Bax/Bcl-2 ratio in ESC tissues isolated from mice-bearing solid Ehrlich tumor.

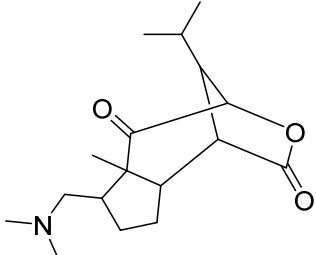
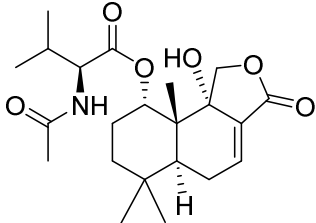
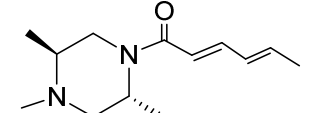
Data (means of three assays) were normalized to the GAPDH mRNA level and expressed as fold induction relative to the mRNA level in the control. Bars, standard deviation and a: significant with respect to the control ($P<0.05$). 5-FU: 5-Fluorouracil (20 mg/kg, i.p.).

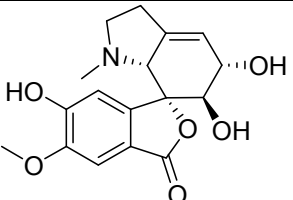
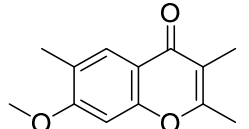
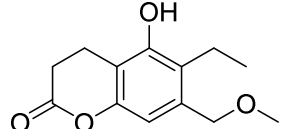
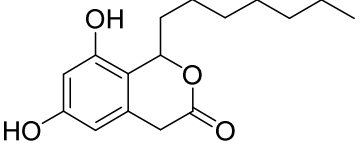
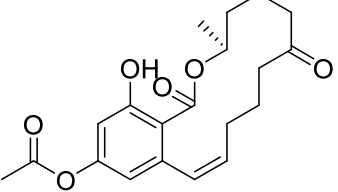
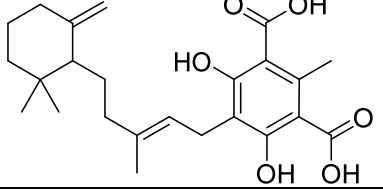
Table 1. Primer sequences of genes analyzed by real time PCR

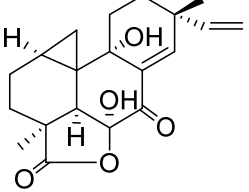
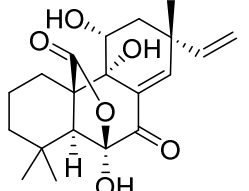
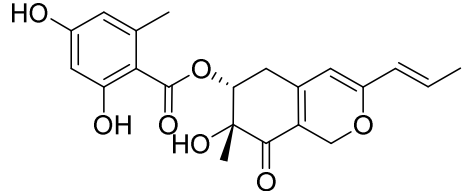
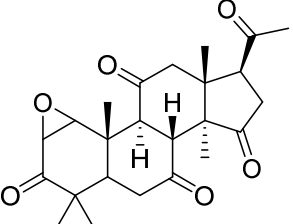
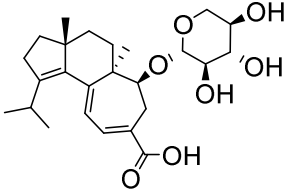
Name	Accession number	Sense (5'---3')	Antisense (5'---3')
GAPDH	NM_017008.4	GCATCTTCTTGTGCAGTGCC	GATGGTGATGGGTTTCCCGT
Bcl-2	NM_016993.1	CTGGTGGACAACATCGCTCTG	GGTCTGCTGACCTCACTTGTG
Bax	NM_017059.2	GGCGAATTGGCGATGAACTG	ATGGTTCTGATCAGCTCGGG
Caspase 3	NM_012922.2	GAGCTTGGAACGCGAAGAAA	TAACCGGGTGCGGTAGAGTA
Bcl-2	NM_016993.1	CTGGTGGACAACATCGCTCTG	GGTCTGCTGACCTCACTTGTG

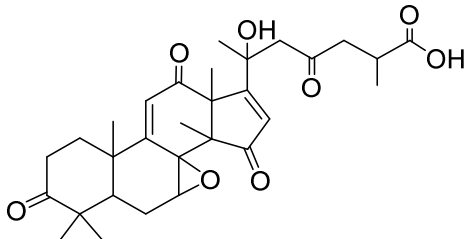
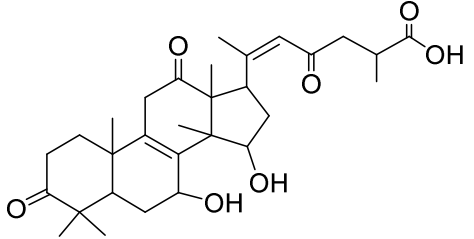
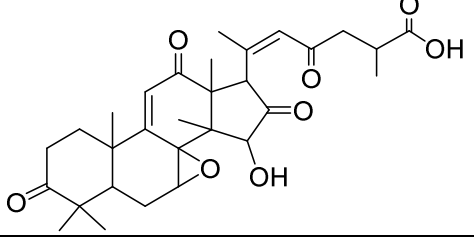
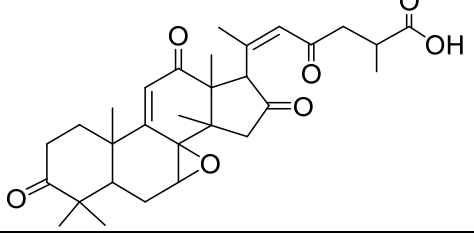
Abbreviations; SOD2: Manganese-dependent superoxide dismutase (MnSOD); CAT: Catalase; GPx1: Glutathione peroxidase 1.

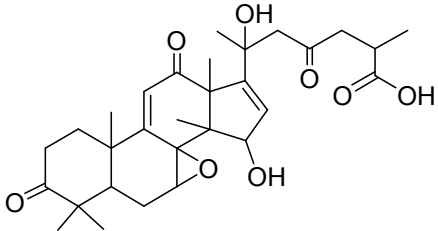
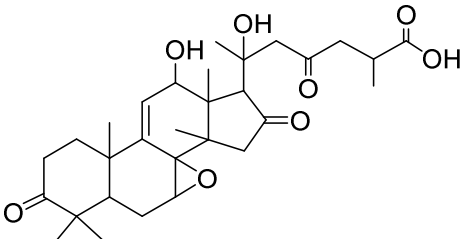
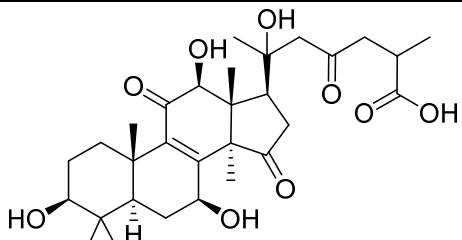
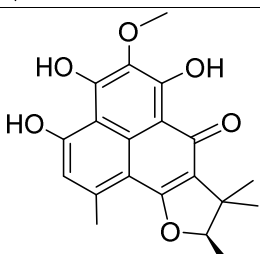
Table 2. LC-HRESIMS analysis of *G. applanatum* extract.

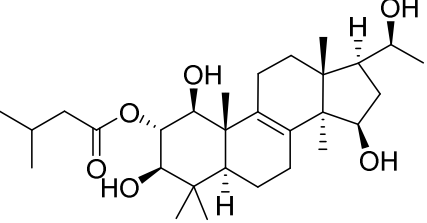
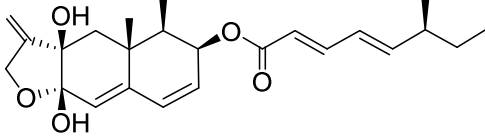
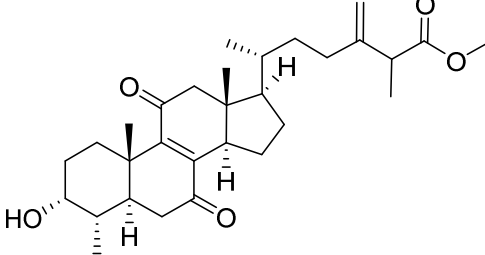
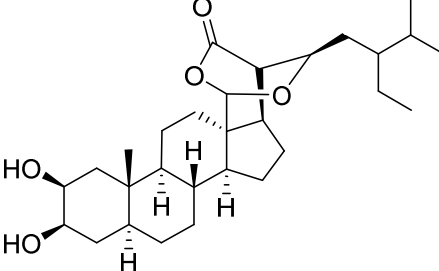
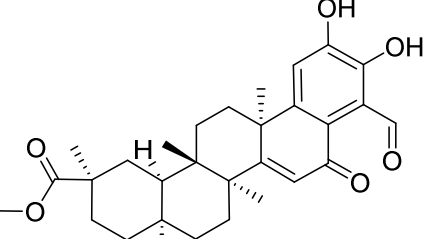
Accurate <i>m/z</i>	Quasi-form	Suggested formula ^a	Tentative identification ^b	Structure	Chemical class	Activity
294.20544	[M+H] ⁺	C ₁₇ H ₂₇ NO ₃	Nobilonine		Alkaloid	No reported activity
408.23779	[M+H] ⁺	C ₂₂ H ₃₃ NO ₆	berkedrimane B		Alkaloid	Cytotoxic [30]
223.18076	[M+H] ⁺	C ₁₃ H ₂₂ N ₂ O	Niragillin		Alkaloid	No reported activity

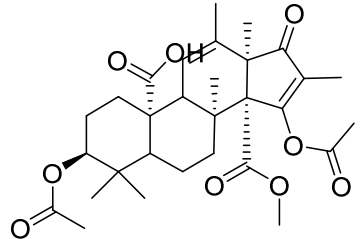
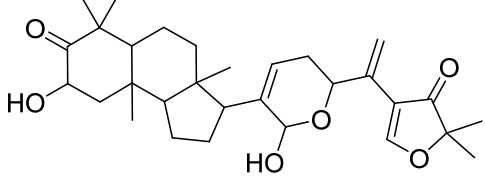
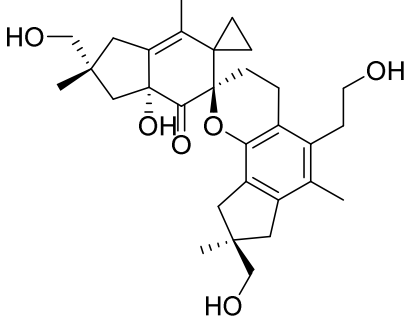
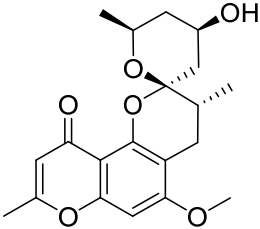
334.12863	[M+H] ⁺	C ₁₇ H ₁₉ NO ₆	8-demethoxyhostasine		Alkaloid	Antiviral
219.10173	[M+H] ⁺	C ₁₃ H ₁₄ O ₃	7-Methoxy-2,3,6-trimethylchromone		Isocoumarin	Cytotoxic [31]
237.11234	[M+H] ⁺	C ₁₃ H ₁₆ O ₄	5-Hydroxy-6-ethyl-7-methoxy-methylchromanone		Isocoumarin	No reported activity
279.15927	[M+H] ⁺	C ₁₆ H ₂₂ O ₄	Cytosporone C		Coumarin	Antimicrobial
361.16507	[M+H] ⁺	C ₂₀ H ₂₄ O ₆	4-Acetyl cis-zearalenone		Terpene	Mycotoxin
417.22675	[M+H] ⁺	C ₂₄ H ₃₂ O ₆	Presiccanochromenic acid		Terpene	No reported activity

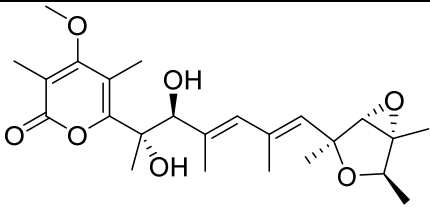
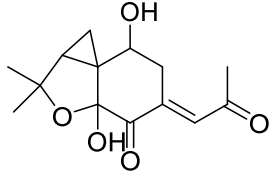
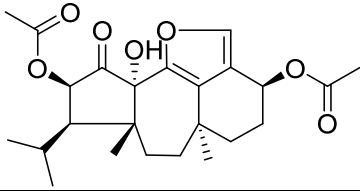
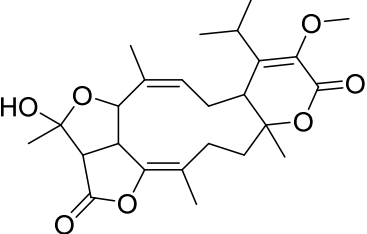
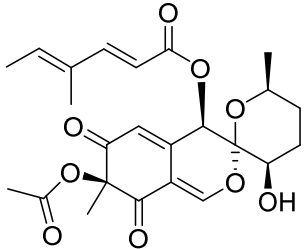
345.16977	[M+H] ⁺	C ₂₀ H ₂₄ O ₅	Myrocin C		Terpene	Antimicrobial
363.18030	[M+H] ⁺	C ₂₀ H ₂₆ O ₆	Sphaeropsidin D		Terpene	Cytotoxic [32]
387.14383	[M+H] ⁺	C ₂₁ H ₂₂ O ₇	Comazaphilone D		Terpene	Antibacterial
415.21146	[M+H] ⁺	C ₂₄ H ₃₀ O ₆	Epoxy-4,4,14-trimethyl-3,7,11,15,20-pentaoxo-pregnane		Terpene	No reported activity
449.25339	[M+H] ⁺	C ₂₅ H ₃₆ O ₇	Erinacine H		Terpene	Nerve growth factor stimulator

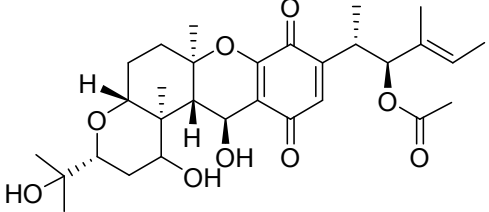
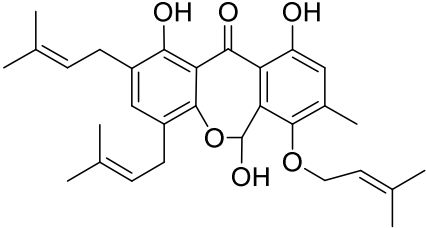
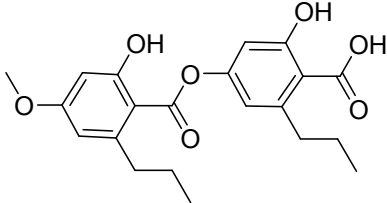
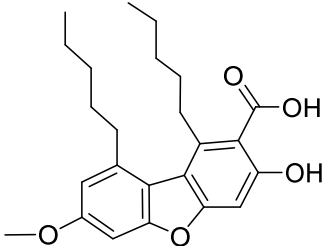
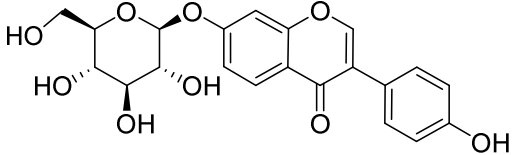
527.26349	[M+H] ⁺	C ₃₀ H ₃₈ O ₈	Applanoxidic acid C		Terpene	Antitumor [33]
515.29987	[M+H] ⁺	C ₃₀ H ₄₂ O ₇	Applanoxidic acid D		Terpene	Antitumor [34]
513.28430	[M+H] ⁺	C ₃₀ H ₄₀ O ₇	Applanoxidic acid E		Terpene	Antioxidant
511.26877	[M+H] ⁺	C ₃₀ H ₃₈ O ₇	Applanoxidic acid F		Terpene	Antitumor [33]

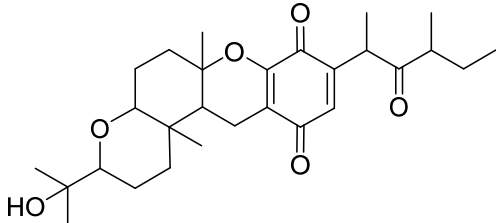
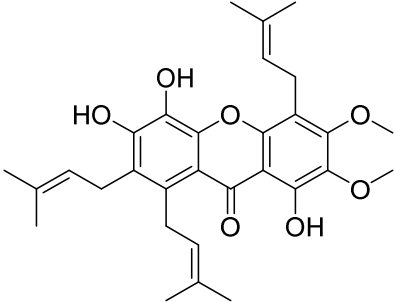
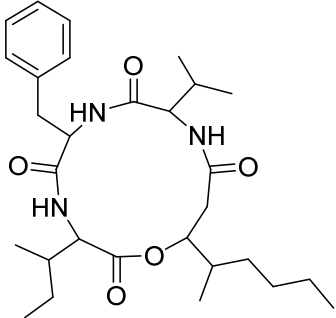
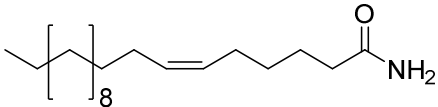
529.27917	[M+H] ⁺	C ₃₀ H ₄₀ O ₈	Applanoxidic acid G		Terpene	Antitumor [33]
531.29480	[M+H] ⁺	C ₃₀ H ₄₂ O ₈	Applanoxidic acid H		Terpene	No reported activity
549.30524	[M+H] ⁺	C ₃₀ H ₄₄ O ₉	20-Hydroxylganoderic acid G		Terpene	No reported activity
357.13345	[M+H] ⁺	C ₂₀ H ₂₀ O ₆	Deoxyherqueinone		Terpene	Antimicrobial

493.35190	[M+H] ⁺	C ₂₉ H ₄₈ O ₆	Xylariacin B		Terpene	Cytotoxic [35]
401.23218	[M+H] ⁺	C ₂₄ H ₃₂ O ₅	Dendryphiellin E		Terpene	No reported activity
485.32584	[M+H] ⁺	C ₃₀ H ₄₄ O ₅	Camphoratin E		Terpene	anti-inflammatory, cytotoxic [36]
475.34146	[M+H] ⁺	C ₂₉ H ₄₆ O ₅	Trichiol C		Terpene	Cytotoxic [37]
495.27344	[M+H] ⁺	C ₃₀ H ₃₈ O ₆	Zeylasteral		Terpene	Antimicrobial

545.27386	[M+H] ⁺	C ₃₀ H ₄₀ O ₉	Citreohybridone E		Terpene	No reported activity
499.30515	[M+H] ⁺	C ₃₀ H ₄₂ O ₆	Sodagnitin A		Terpene	No reported activity
497.28922	[M+H] ⁺	C ₃₀ H ₄₀ O ₆	Bovistol		Terpene	No reported activity
361.16470	[M+H] ⁺	C ₂₀ H ₂₄ O ₆	Chaetoquadrin A		Polyketide	Antifungal

435.23755	[M+H] ⁺	C ₂₄ H ₃₄ O ₇	Verrucosidinol		Polyketide	No reported activity
267.12311	[M+H] ⁺	C ₁₄ H ₁₈ O ₅	Papyracon A		Polyketide	Antimicrobial
433.22171	[M+H] ⁺	C ₂₄ H ₃₂ O ₇	Heptemerone D		Polyketide	Cytotoxic [38]
447.23749	[M+H] ⁺	C ₂₅ H ₃₄ O ₇	Atranone B		Polyketide	phytotoxic
461.18042	[M+H] ⁺	C ₂₄ H ₂₈ O ₉	Daldinin F		Polyketide	Antioxidant

547.28943	[M+H] ⁺	C ₃₀ H ₄₂ O ₉	Stemphone B		Polyketide	Anti-MRSA
493.25800	[M+H] ⁺	C ₃₀ H ₃₆ O ₆	Arugosin G		Polyketide	No reported activity
389.15979	[M+H] ⁺	C ₂₁ H ₂₄ O ₇	Divaricatic acid		Polyketide	Antimicrobial
399.21658	[M+H] ⁺	C ₂₄ H ₃₀ O ₅	Condidymic acid		Polyketide	No reported activity
417.11819	[M+H] ⁺	C ₂₁ H ₂₀ O ₉	7-O-Glucosyl-daidzein		Isoflavonoid	Different bioactivities

473.28958	[M+H] ⁺	C ₂₈ H ₄₀ O ₆	14-Epicochloquinone B		Xanthone	Antibacterial
509.25305	[M+H] ⁺	C ₃₀ H ₃₆ O ₇	nujiangexanthone B		Xanthone	Cytotoxic [39]
516.34253	[M+H] ⁺	C ₂₉ H ₄₅ N ₃ O ₅	Beauverolide E		Peptide	No reported activity
338.34201	[M+H] ⁺	C ₂₂ H ₄₃ NO	6-cis-docosenamide		Fatty amide	No reported activity
451.23224	[M+H] ⁺	C ₂₄ H ₃₄ O ₈	No hits		Terpene	
530.31036	[M+H] ⁺	C ₃₀ H ₄₃ NO ₇	No hits		steroidal alkaloid	

^a High Resolution Electrospray Ionization Mass Spectrometry (HRESIMS) using XCalibur 3.0 and allowing for M+H / M+Na adduct.

^b The suggested compound according to Dictionary of Natural Products (DNP 23.1, 2015 on DVD) and Reaxys online database.

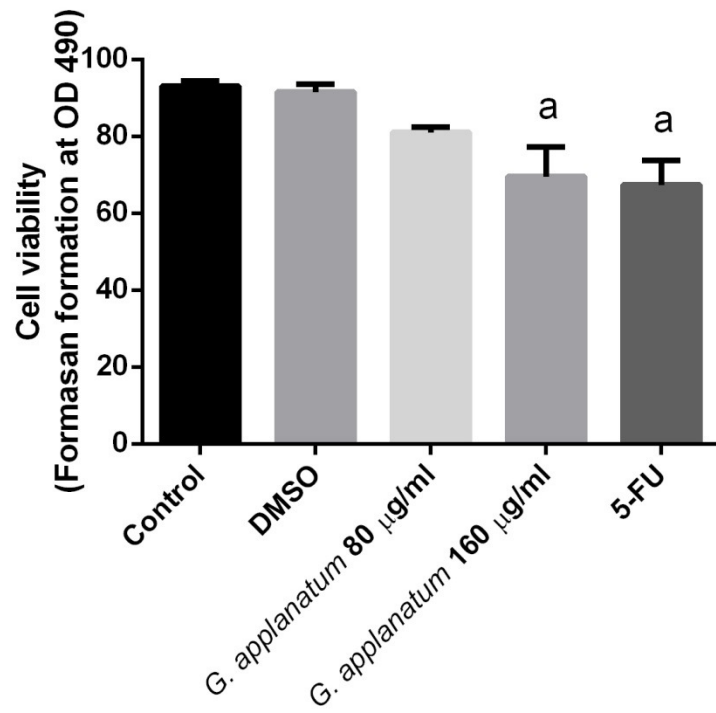


Figure 1. Assessment of cell viability and morphological changes by acridine orange/ethidium bromide (AO/EB) dual fluorescent staining.

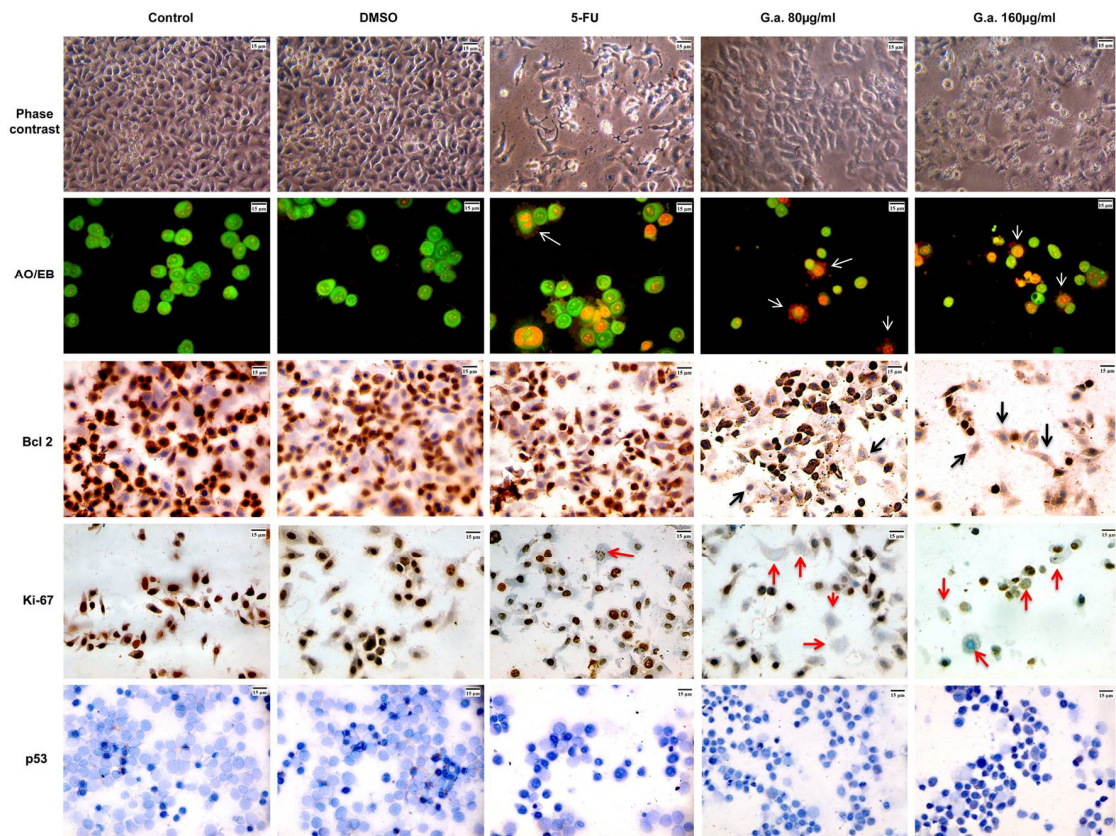


Figure 2. Morphological changes observed by inverted microscope (phase contrast); detected by acridine orange/ethidium bromide (AO/EB) dual fluorescent staining

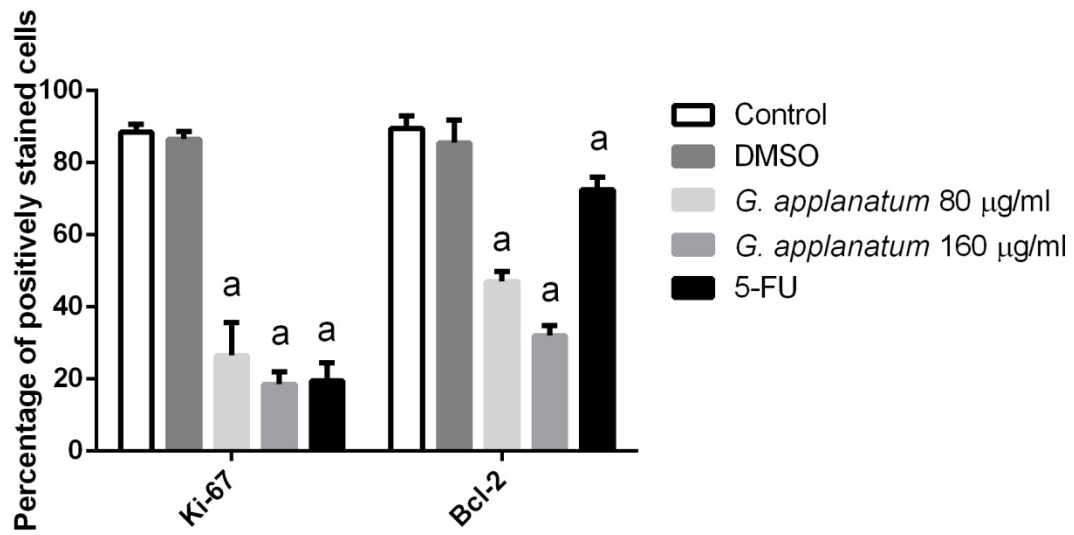


Figure 3. Percentage of protein expression (positively stained cells) of Bcl-2 and Ki-67 detected by immunocytochemistry in control and treated Caco-2 cells after 24 hrs.

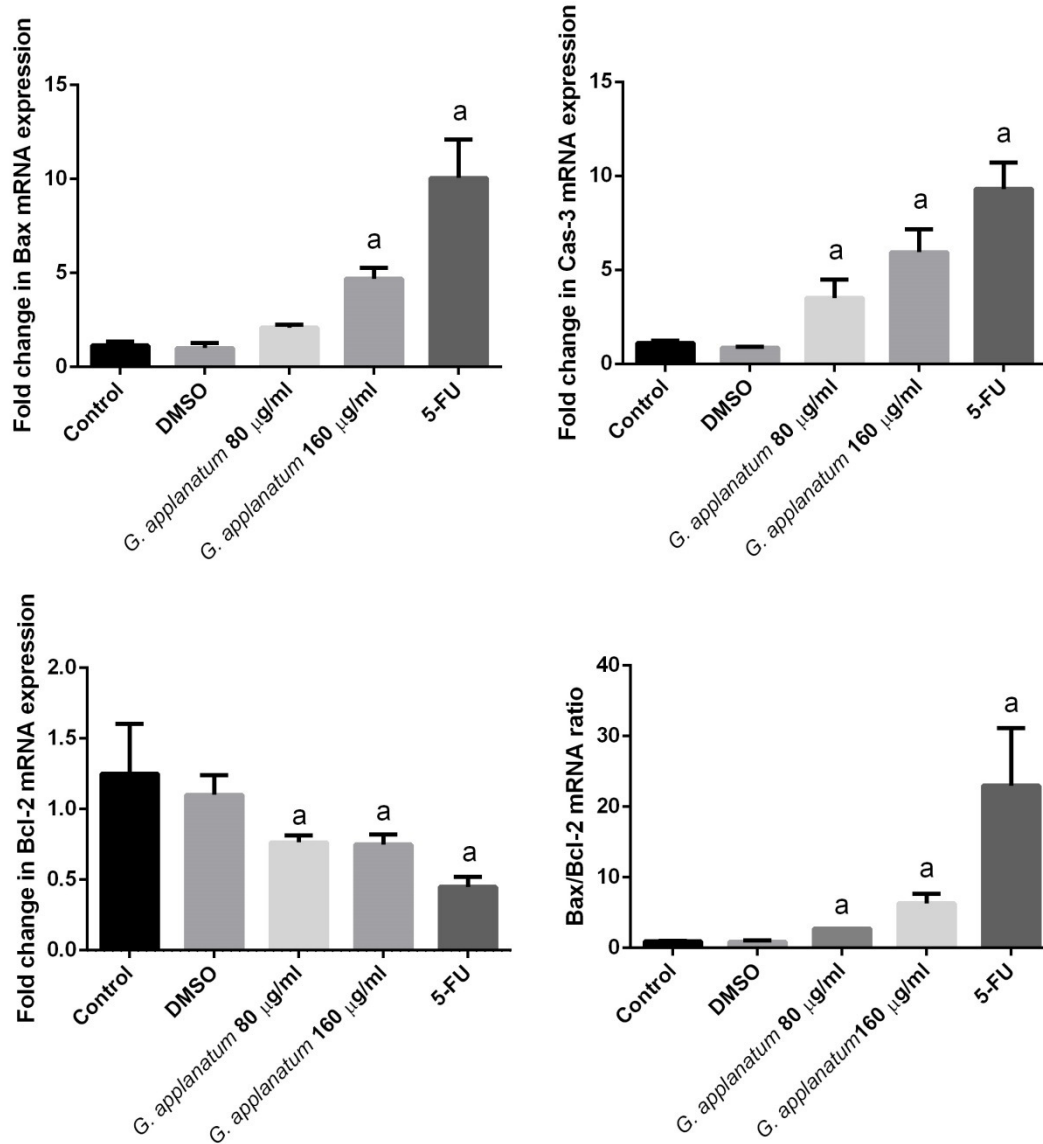


Figure 4. The relative mRNA alterations of Bax, Cas-3 and Bcl-2 expression were quantified in control and treated Caco-2 cells using quantitative real-time PCR,

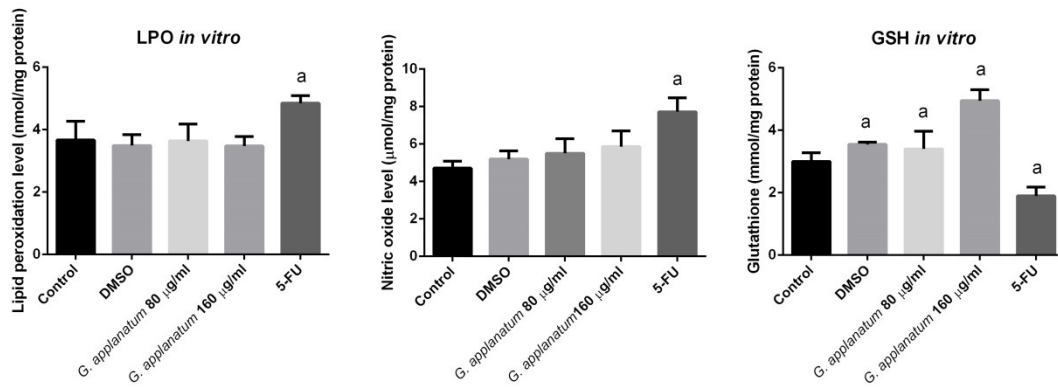


Figure 5. Lipid peroxidation (LPO), nitric oxide (NO) and glutathione (GSH) levels in control and treated Caco-2 cells after 24 hrs.

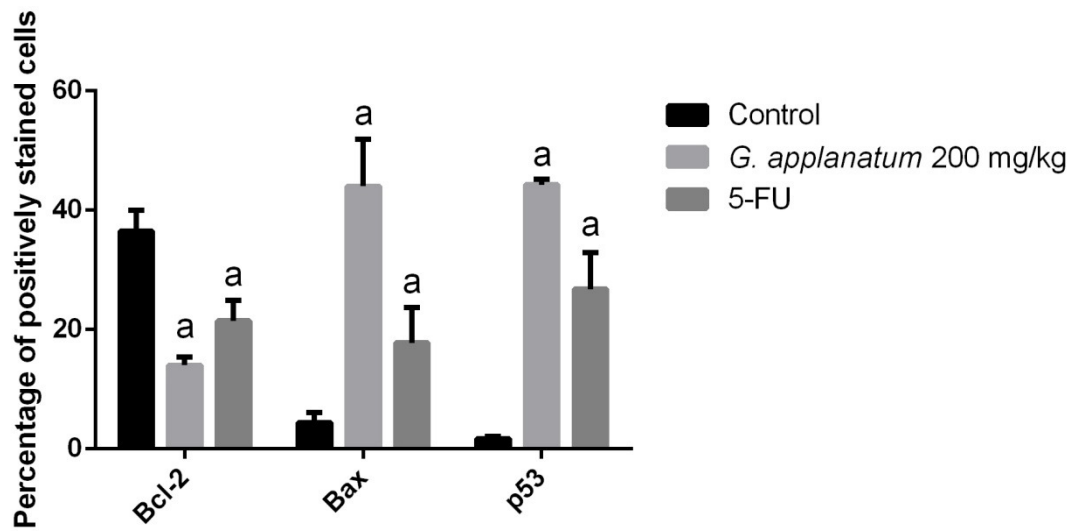


Figure 6. Marked decrease in solid Ehrlich tumor volume after five days of different treatments.

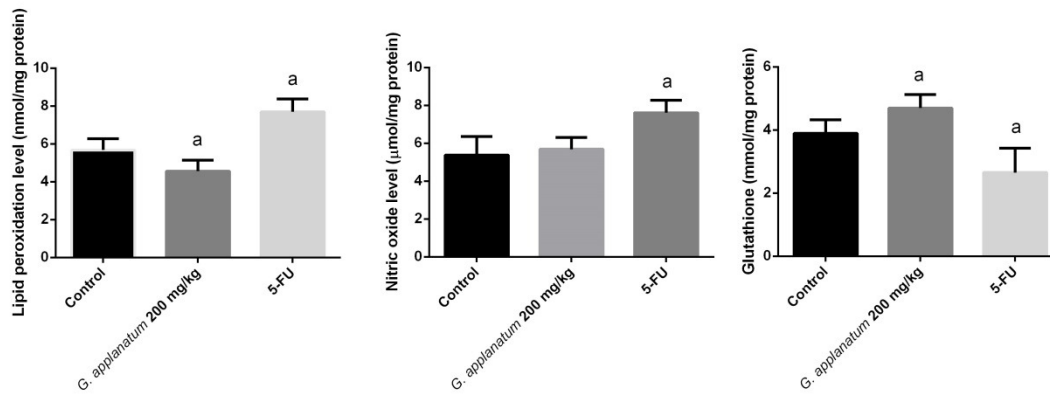


Figure 7. Effect of *G. applanatum* (200 μg/ml) treatments on lipid peroxidation (LPO), nitric oxide (NO) and glutathione (GSH) levels in solid Ehrlich tumor tissues after 4 days of different treatments.

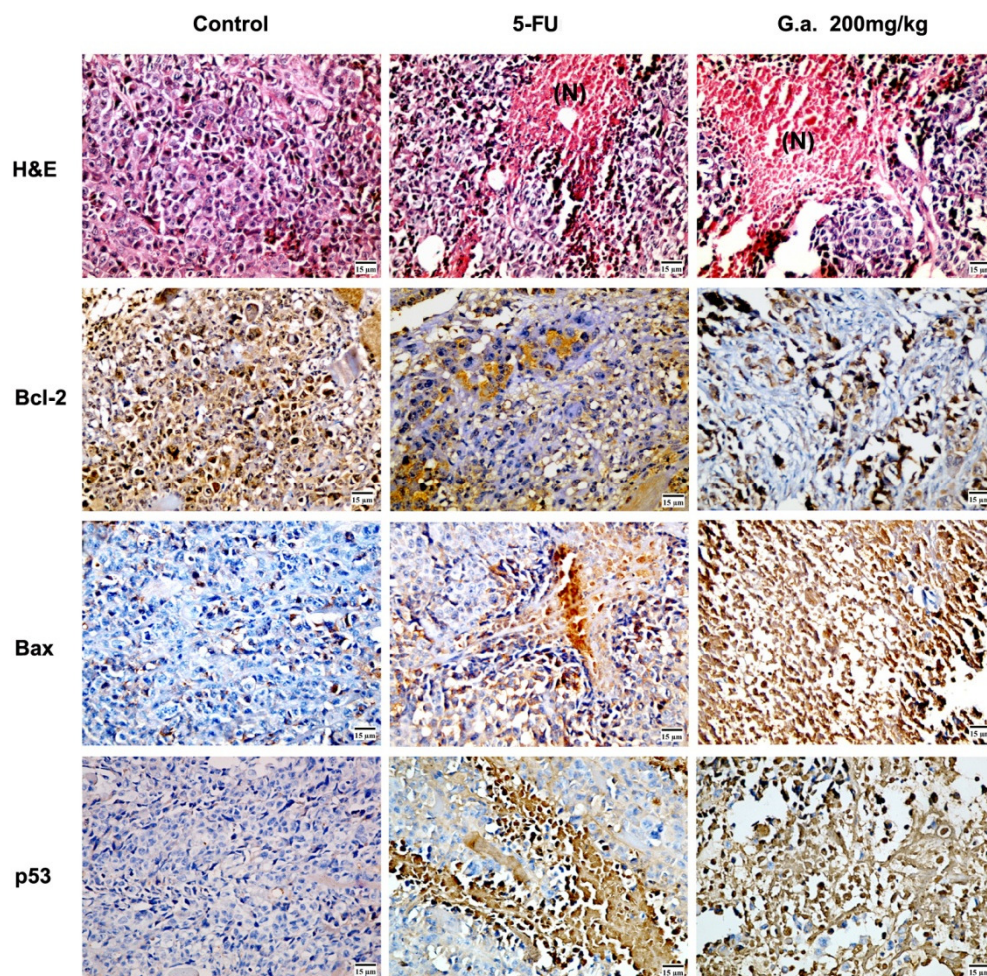


Figure 8. Representative photomicrographs of control and treated solid Ehrlich tumor sheets.

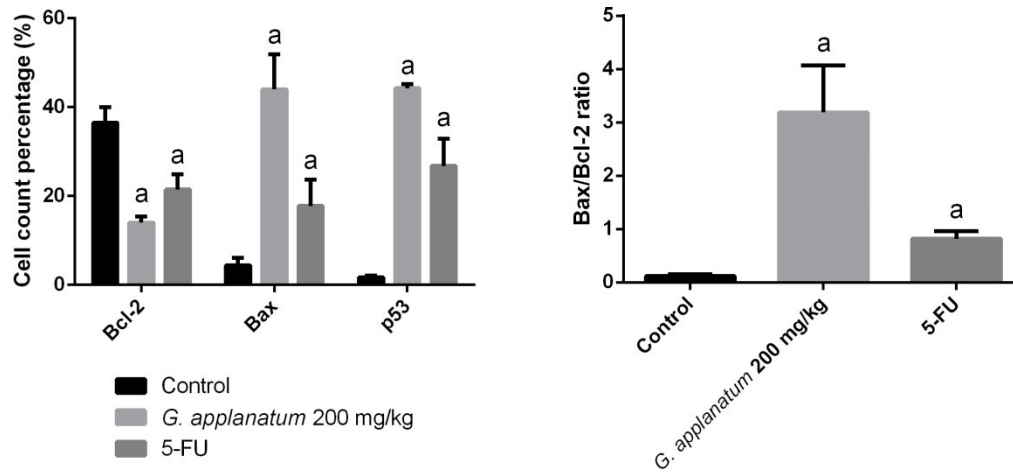


Figure 9. Percentage of protein expression (positively stained cells) of Bcl-2, Bax and p53 as detected by immunocytochemistry in control and treated mice-bearing SEC tissues.

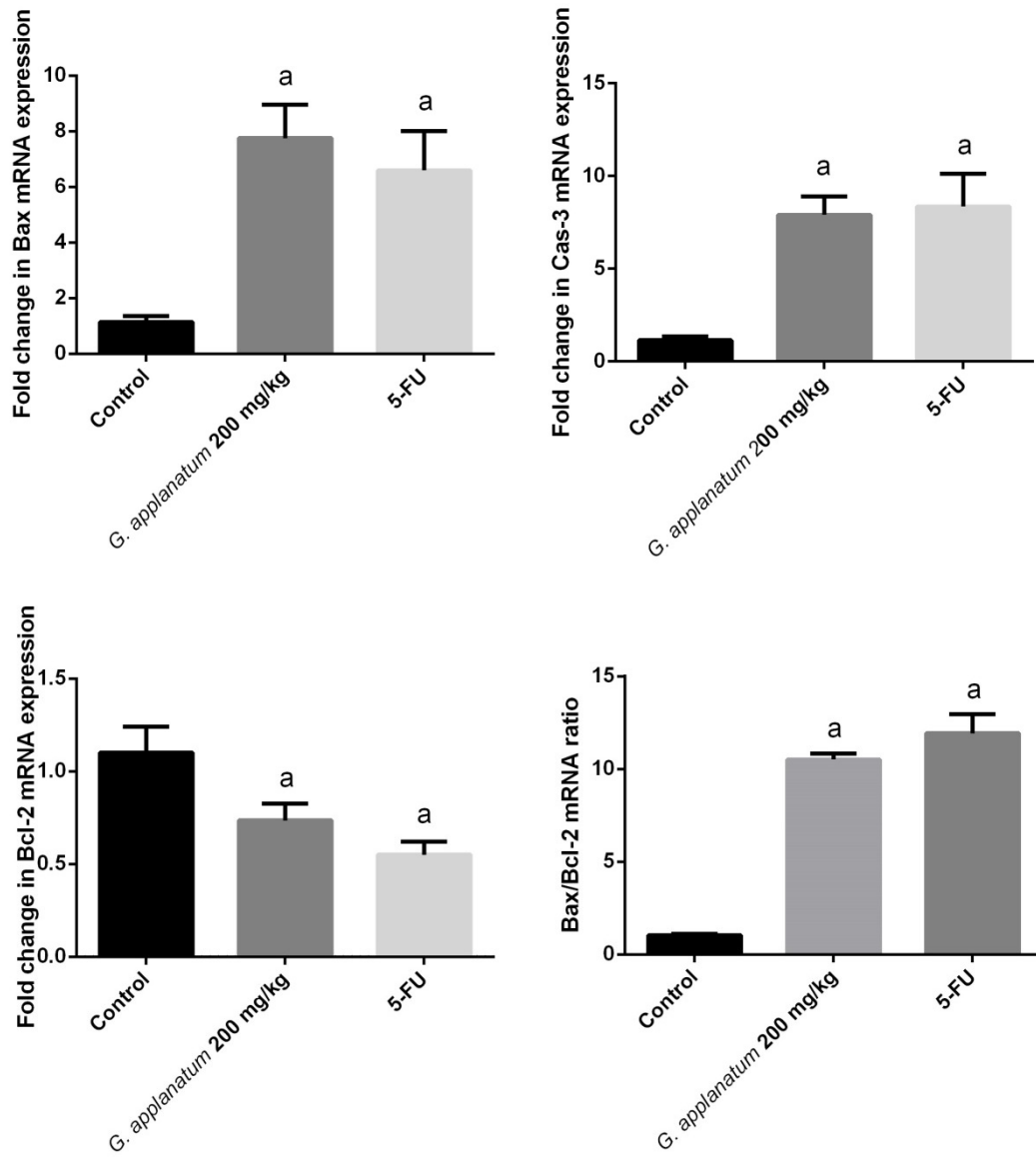


Figure 10. The relative mRNA alterations of Bax, Cas-3 and Bcl-2 expressions.